Author Manuscript

Author Manuscript

Author Manuscript

Author Manuscript

HHS Public Access

Author manuscript

J Med Chem. Author manuscript; available in PMC 2017 October 17.

Published in final edited form as:

J Med Chem. 2017 March 09; 60(5): 2018–2025. doi:10.1021/acs.jmedchem.6b01767.

Room temperature neutron crystallography of drug resistant HIV-1 protease uncovers limitations of X-ray structural analysis at 100K

Oksana Gerlits[1], **David A. Keen**[2], **Matthew P. Blakeley**[3], **John M. Louis**[4], **Irene T. Weber**[5], and **Andrey Kovalevsky**[6,*]

[1]UT/ORNL Joint Institute of Biological Sciences, University of Tennessee, Knoxville, TN USA

[2]ISIS Facility, Rutherford Appleton Laboratory, Harwell Campus, Didcot, OX11 0QX, UK

[3]Large-Scale Structures Group, Institut Laue Langevin, 71 avenue des Martyrs, 38000 Grenoble, France

[4]Laboratory of Chemical Physics, National Institute of Diabetes and Digestive and Kidney Diseases, National Institutes of Health, DHHS, Bethesda, Maryland 20892-0520, USA

[5]Departments of Chemistry and Biology, Georgia State University, Atlanta, GA 30302, USA

[6]Biology and Soft Matter Division, Oak Ridge National Laboratory, Oak Ridge, TN 37831, USA

Abstract

HIV-1 protease inhibitors are crucial for treatment of HIV-1/AIDS, but their effectiveness is thwarted by rapid emergence of drug resistance. To better understand binding of clinical inhibitors to resistant HIV-1 protease, we used room-temperature joint X-ray/Neutron (XN) crystallography to obtain an atomic-resolution structure of the protease triple mutant (V32I/I47V/V82I) in complex with amprenavir. The XN structure reveals a D^+ ion located midway between the inner Oδ1 oxygen atoms of the catalytic aspartic acid residues. Comparison of the current XN structure with our previous XN structure of the wild-type HIV-1 protease-amprenavir complex suggests that the three mutations do not significantly alter the drug-enzyme interactions. This is in contrast to the observations in previous 100K X-ray structures of these complexes that indicated loss of interactions by the drug with the triple mutant protease. These findings, thus, uncover limitations of structural analysis of drug binding using X-ray structures obtained at 100K.

Graphical abstract

Corresponding Author Information: To whom correspondence should be addressed: kovalevskyay@ornl.gov, 505-310-4184 (AK).

PDB ID Codes: the joint XN structure of PR_{TM}-APV complex has been deposited to the Protein Data Bank with the code 5T8H. Authors will release the atomic coordinates and experimental data upon article publication.

Author contributions: OG, and AK designed research; OG, and AK performed research; DAK, and MPB collected neutron diffraction data; OG, JML, MPB and AK analyzed data; OG, JML, ITW and AK wrote the paper.

Author Manuscript Author Manuscript Author Manuscript Author Manuscript

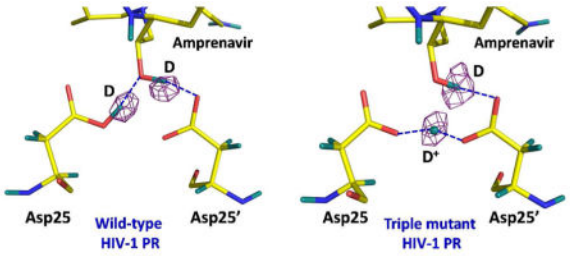

Keywords

HIV-1 protease; drug resistance; joint X-ray/neutron crystallography; hydrogen bonding; hydrophobic interactions

INTRODUCTION

HIV-1/AIDS is a pandemic with no cure. Combination antiretroviral therapy involving treatment with several potent drugs targeting different steps in the viral replication cycle provides a vital treatment option for the individuals infected with HIV-1.[1] HIV-1 protease (PR), a crucial viral enzyme, has proven to be a valuable target for drug design, with nine clinical inhibitors currently marketed in the US.[2,3] The development of the HIV-1 PR inhibitors has been viewed as perhaps one of the best examples of structure-guided drug design.[4] However, the long-term potency of the PR inhibitors is thwarted by rapid emergence of drug resistant PR variants, necessitating constant urge to develop of new drugs that have higher genetic barrier to resistance and that are active against resistant PR variants.[5,6]

The design of PR inhibitors has been guided mainly by low-temperature (100K) X-ray structures of the enzyme-ligand complexes.[7] Moreover, cryo-crystallography has been instrumental in studying the structural basis of drug resistance by comparing and contrasting intermolecular interactions made by inhibitors in the wild-type and drug resistant PRs.[8,9] In the majority of cases, the reduction of an inhibitor's affinity for the PR harboring drug resistant mutations has been attributed to the disappearance or weakening of favorable interactions between the inhibitor's functional groups and side chains of the mutated residues. This is exemplified by the X-ray structures of drug resistant PR variants with various clinical protease inhibitors.[8–12] In a few instances, however, drug resistant mutations lead to possible formation of unfavorable interactions, with a stark example of saquinavir-specific substitution G48V.[10,13]

Although low-temperature X-ray crystallography is an attractive technique for structure determination due to recent advances in synchrotron radiation and automation, diffraction data are collected from crystals cooled to the temperature ~210°C below the physiological temperature. In addition, crystals need treatment with cryo-protecting solutions and are flash-frozen in liquid nitrogen at non-equilibrium conditions prior to X-ray exposure. Thus, cryo-cooling may lead to systematic distortion of the repertoire of accessible conformations of a protein at low temperature relative to room temperature.[14–16] This can lead to incorrect

Author Manuscript Author Manuscript Author Manuscript Author Manuscript

inferences about the functional roles of specific protein groups either in enzyme catalysis or ligand binding.

We recently used room temperature joint X-ray/Neutron (XN) crystallography to obtain an atomic-level picture of clinical drug amprenavir (APV) binding to the wild-type HIV-1 PR, PR_{WT}-APV (Figure 1A and 1B; PDB ID 4JEC).[17] We capitalized on the unique ability of neutron diffraction to directly locate hydrogen (and deuterium) atoms in macromolecules to visualize hydrogen bonding and hydrophobic interactions made by the protease inhibitor with the main-chain and side-chain atoms of the enzyme active site cavity, and demonstrated that some interactions previously inferred from the low-temperature X-ray structure[11,18] were either significantly weaker or did not form at all. In this work, we report a room temperature XN structure of the PR triple mutant variant V32I/I47V/V82I (referred to as PR_{TM} henceforth) in complex with APV at pH 6.0 (PDB ID 5T8H), and compare it to the room temperature XN structure of PR_{WT}-APV complex[17] and to the low temperature PR_{TM}-APV X-ray structure.[19] Importantly, we observe that cryo-cooling results in “freezing out” of side-chain conformations, not detected at room temperature, for drug resistant mutations, possibly biasing the interpretation of the structural roles of these mutations in drug resistance. In addition, the XN structure of PR_{TM}-APV unambiguously shows a D^+ ion positioned half-way between the inner oxygen atoms of the catalytic Asp25 and Asp25′ carboxylic groups, taking part in a possible low-barrier hydrogen bond – an observation that would not be possible with X-rays.

RESULTS and DISCUSSION

Deuterium atom locations and protonation states

The X-ray scattering power of hydrogen (H) is weak, and it is dependent on the electron density present on H, being decreased further for more acidic H atoms. To observe H atoms in X-ray structures diffraction data to resolutions better than 1 Å are generally obtained. The neutron scattering power of H (−3.739 fm), and its heavier isotope deuterium (D, 6.671 fm), is as good as that of carbon (6.646 fm), oxygen (5.803 fm) and nitrogen (9.360 fm), and is independent from the chemical environment. Yet, H possesses the negative neutron scattering length, causing cancellation effects in the nuclear density maps, and also has a strong incoherent scattering component that contributes heavily to the background. Thus, H is usually exchanged with D in protein crystals to increase signal-to-noise ratio and improve neutron diffraction. Locating D atoms in nuclear density maps is straightforward, even at resolutions as low as 2.5 Å.[20] In case of HIV-1 PR studied here, in addition to substituting D for H at the exchangeable sites, we replaced H in C-H bonds with D by expressing the enzyme in D_2O, which further improves the quality of neutron diffraction signal and allows us to use crystals of ~0.2 mm^3, the crystal volume considered small by macromolecular neutron crystallography standards. The structures are refined against two diffraction datasets – neutron and X-ray – collected preferably from the same crystal in a joint refinement strategy,[21] resulting in more accurate structures that as described as XN structures henceforth.

Crucial for our detailed structural analysis, only one orientation of APV is observed in the active site of the per-deuterated enzyme. The lack of the drug disorder, which is common in

Author Manuscript Author Manuscript Author Manuscript Author Manuscript

the X-ray structures of PR complexes with inhibitors, makes it possible to determine positions of D atoms with high confidence. Previously, the observation of DRV disordered over two orientations by a 180° flip did not allow us to observe any H atoms in the 0.84 Å ultra-high resolution X-ray structure of V32I PR variant in complex with DRV,[22] for many residues showed disorder as well, including main-chain atoms and the catalytic site.

The catalytic Asp25/Asp25′ dyad in HIV-1 PR is expected to be monoprotonated in the pH range 5–6.[23–26] In the XN structure of PR_{TM}-APV complex at pH 6.0 we found one D atom in the catalytic site (Figure 2A). Remarkably, the D atom is observed as a D^+ (deuterium ion), positioned between the inner Oδ1 oxygen atoms of the two aspartic acid residues, and possibly involved in a strong low-barrier hydrogen bond. The D^+ is essentially equally distanced from the oxygen atoms, with the D···O distances of 1.5–1.6 Å, but it is farther away from the hydroxyl oxygen of APV (2.0 Å) (Figure 2B). Therefore, the D^+ is weakly coordinated with the OD of APV. In our previous XN structure of PR_{WT}-APV,[17] however, this D atom is covalently bound to the Oδ1 oxygen of Asp25 and makes a strong hydrogen bond of 1.5 Å with the oxygen of APV hydroxyl (Figure S1). In both XN structures the OD of APV is rotated to Asp25′ and forms a 1.7 Å hydrogen bond with the outer Oδ2 oxygen. Consequently, the overall interaction of APV with the catalytic residues in PR_{TM} may be weaker than in PR_{WT}, which may contribute to the 15-fold lower affinity of APV to PR_{TM}.[19] The formation of the low barrier hydrogen bond between Asp25 and Asp25′ was previously found in molecular simulations[27–29] and QM/MM calculations[30] of the apo- and substrate-bound PR. It has also been proposed that such a strong hydrogen bond is an important feature of the HIV-1 PR catalytic mechanism, and that it may be common for other aspartic proteases.[31] Importantly, our current study is the first one to directly observe a D^+ between the catalytic aspartates for any aspartic protease.

It is of note that in our earlier XN structure of PR_{TM} in complex with darunavir (DRV) at pH 6.0, the catalytic site D was also observed as D^+, but unlike in PR_{TM}-APV, it is shared between the carboxylic group of Asp25′ and the hydroxyl of DRV (Figure S1).[32] The D^+ is located equally distanced from Oδ1 and Oδ2 of Asp25′, and hydroxyl oxygen of DRV. Additionally, the catalytic site D is located at the outer Oδ2 oxygen of Asp25 in the XN structure of PR_{TM}-DRV at pH 4.3, the position where it would be ready to attack the carbonyl oxygen of a substrate in a PR-substrate complex,[24] and forms a very weak hydrogen bond with the hydroxyl of DRV. The positioning of the D atom on the outer Oδ2 oxygen of the catalytic aspartic acid in PR_{TM}-DRV at pH 4.3 is similar to that in the pH 5.0 neutron structure of wild-type PR in complex with a non-clinical inhibitor.[33] It appears that an external stimulus is required to shift the location of the catalytic dyad D to one of the outer Oδ2 carboxylic oxygens. In that non-clinical inhibitor[33] the electrostatics of the carbonyl group vicinal to the inhibitor hydroxyl drives the catalytic dyad D positioning on Oδ2 to form a strong hydrogen bond and to avoid a repulsive interaction between the two partially negatively charged oxygen atoms. On the other hand, long-range electrostatics triggers transfer of D to the Oδ2 of Asp25 when the pH is lowered to 4.3 in the crystal of PR_{TM}-DRV.[32] Taken together, the observations of the positions of hydrogen atoms in the XN structures of HIV-1 PR described above demonstrate that the catalytic site deuteron is labile and can occupy all possible positions within the confines of the catalytic residues and hydroxyl groups of inhibitors.

Author Manuscript Author Manuscript Author Manuscript Author Manuscript

Mutations do not alter interactions in PR_{TM}-APV relative to PR_{WT}-APV according to XN structures

Direct observation of D atoms in PR and inhibitors is crucial to make correct interpretation of the drug-enzyme interactions, including hydrogen bonds and hydrophobic contacts. APV binding mode is identical in PR_{TM} and PR_{WT} in the room temperature XN structures, with similar hydrogen bonding interactions (Figure 3). Thus, mutations of the hydrophobic residues at positions 32, 47 and 82 do not appear to dramatically disrupt the hydrogen bonding pattern, except for the weaker interaction of the catalytic site D with the hydroxyl of APV in PR_{TM}-APV. In both XN structures the strongest hydrogen bonds are made by the hydroxyl group of APV with the catalytic Asp25′. In addition to interacting with the catalytic site, APV makes two more direct hydrogen bonds, with the backbone amides of residues Asp30, and Asp30′ at the opposite ends of the drug. These hydrogen bonds are rather weak, however, as the D···O and D···N distances are 2.3–2.5Å, but they are not altered by the three mutations in PR_{TM}. Several additional interactions suggested by the previous low temperature X-ray structures[11,19] are probably insignificant, even though distances between the heavy atoms would indicate hydrogen bonding. In particular, in both XN structures the N-D group of APV carbamate is almost perpendicular to the plane of the main-chain carbonyl of Gly27. Similarly, the flap water plane is perpendicular to the backbone N-D bond of Ile50′ (Figure S2); thus, the water's lone pair of electrons is not directed toward the D atom. This observation suggests that the drugs are not symmetrically bound to the flaps, which appears to be in accord with the previous NMR studies[34] that demonstrated asymmetry in the flaps' opening and closing dynamics. In addition, the main-chain N-D of Asp29 makes a ~120° angle with the oxygen of the tetrahydrofuran ring. The geometry of these contacts deviates significantly from the canonical values for hydrogen bonding; thus, they cannot be considered as such. On the other hand, because the N-D vector of the APV carbamate is perpendicular to π system of the main-chain carbonyl of Gly27 this interaction can be considered a weak N-D···π contact, with the D···π and N···π distances to the center of the C=O double bond in both XN structures of 2.6 and 3.5 Å, respectively.

The superposition of PR_{WT}-APV and PR_{TM}-APV XN structures depicting the mutation sites and hydrophobic interactions is shown on Figure 4. The two XN structures superpose with an RMS deviation of 0.16 Å on the backbone atoms. From a detailed analysis of the two XN structures it is evident that drug resistant substitutions V32I, I47V and V82I, which add or remove a CH_3 group on the side chains, do not significantly alter the hydrophobic contacts. Specifically, in PR_{TM}-APV the aniline group of APV makes C-H···π interactions with the side chains of V47 and I32, with the C···C distances of 3.4–3.9 Å. The corresponding distances for C-H···π contacts are 3.6–4.0Å in PR_{WT}-APV. In addition, C-H···π interactions are made by the benzyl group of APV with the side chains of residue 82, with the C···C distances of 3.7–4.0 Å in PR_{TM}-APV and 3.4–3.9 Å in PR_{WT}-APV. We use here C···C distances to describe C-H···π interactions because it has been demonstrated by NMR[35] that the C-H···π interaction strength involving aliphatic groups and aromatic rings is mainly determined by the distances between their carbon atoms, while lateral displacement of a C-H group away from pointing directly at the center of the π system does not greatly affect the interaction if the C···C separation is ≤ 4.0 Å. The isobutyl and tetrahydrofuran groups make similar closed-shell van der Waals interactions with side chains of residues 32, 47 and 82,

Author Manuscript Author Manuscript Author Manuscript Author Manuscript

with C···C distances of 3.6–4.1 Å and 3.7–4.1 Å in PR_{TM}-APV and PR_{WT}-APV, respectively.

Side chains have different conformations in 100K X-ray and room temperature XN structures of PR_{TM}-APV

The common practice used to understand the structural role of drug resistant mutations is to compare low temperature X-ray structures of wild-type and mutant PR in complex with drugs. The 15-fold lower affinity of APV to PR_{TM} compared to PR_{WT} has been previously explained by the loss of hydrogen bonding between the drug's aniline moiety and Asp30′ and by the weakening of hydrophobic interactions such as van-der-Waals contacts between the tetrahydrofuran group and the side chain of residue 32, and C-H···π interactions between the aniline moiety and the side chain of residue 47′ as observed in the 100K X-ray structure of PR_{TM}-APV compared to the 100K X-ray structure of PR_{WT}-APV.[19]

The 100K X-ray and the room temperature XN structures of PR_{TM}-APV superimpose with the low RMS deviation on the main chain atoms of 0.25 Å. However, a number of side-chains, including those at the mutation sites, show different conformations at room temperature relative to those at 100K. Strikingly, the aniline of APV is disordered at 100K by bending at sulfur of sulfonamide, while at the same time, Asp30′ side chain shows disorder over two conformations, seemingly in concert with the aniline group bending (Figure 5). In the room temperature XN structure, however, no disorder of these groups is observed, with Asp30′ and aniline superimposing onto one of the conformations observed at 100K in the X-ray structure. A water molecule is also visible in the neutron structure connecting aniline's ND_2 group to the carboxylate of Asp30′. Unexpectedly, we observe that the side chains of I32 and V47′ are rotated by about 120 ° in the 100K X-ray structure relative to their conformations in the room temperature XN structure (Figure 5). In the room temperature XN structure I32 and V47′ are involved in van der Waals and C-H···π interactions, respectively, with APV as described in detail above, but these contacts are apparently diminished in the 100K X-ray structure. Specifically, the number of van der Waals contact between the I32 side chain and the tetrahydrofuran group decreases and they lengthen to > 3.8 Å, whereas C···C distances from the V47′ side chain to the aromatic carbon atoms of the major aniline conformation are increased to > 4.5 Å. Also, in the 100K X-ray structure Ile32′ is disordered over two conformations, one of which retaining C-H···π interactions with aniline, whereas Val47 has identical conformation to that in the room temperature XN structure.

It is important to emphasize, therefore, that evidently one must be careful when comparing 100K X-ray structures of the wild-type and mutant PR in complex with drugs with the aim of analyzing the effects of drug resistant mutations on the non-covalent interactions. Also, our comparison of the room temperature XN structures of PR_{WT}-APV and PR_{TM}-APV complexes reveals that some mutations may not lead to clear observation in the crystal structures of significant structural changes that weaken hydrogen bonding and hydrophobic interactions; thus, changes in other PR properties such as in its global dynamics and conformational flexibility due to introduction of the drug resistant mutations may provide a significant contribution to the drug resistance of such PR variants. The PR dynamics would

Author Manuscript Author Manuscript Author Manuscript Author Manuscript

contribute to the order/disorder of the system, and thus contribute to the entropy of the system. To find out whether there are differences in the ΔS of APV binding to PR_{TM} we performed ITC measurements comparable to conditions used for the XN structure (Figure S3) and compared them to those corresponding to APV binding to PR_{WT}.[36] The slightly less favorable ΔH of APV binding to PR_{TM} (Table S2) can be explained by the weakening of hydrogen bonding between the APV hydroxyl and the catalytic residues, as discussed above. More interestingly, the ΔS of APV binding to PR_{TM} is significantly smaller (ΔΔS of ca. −4 cal/mol·K) than that of the drug binding to PR_{WT}. It follows that PR_{TM}-APV complex has fewer degrees of freedom compared to PR_{WT}-APV. If we assume that other properties contributing to ΔS, such as desolvation of APV and the PR active site upon drug binding, are very similar for the wild-type and mutant enzymes, then we can hypothesize that such unfavorable ΔΔS may indicate stiffened dynamics of PR_{TM} relative to that of PR_{WT}. In fact, previous molecular dynamics simulations have shown that some mutations may result in lower conformational flexibility of the protease mutants.[37] Other molecular dynamics simulations and a number of NMR studies have demonstrated that drug resistant mutations distal to the drug binding cavity are capable of altering the PR dynamics, including the flap dynamics, and conformational sampling.[38–43] For example, the highly resistant mutant PR20 bearing 19 naturally evolved drug resistant mutations exhibits altered flap conformations and an expanded binding cavity.[12] Other factors, such as long range electrostatics, solvent effects, etc. can also be contributing factors that cannot be easily assessed in crystal structures or by ITC.

CONCLUSIONS

Macromolecular neutron crystallography has given us an unprecedented picture of the atomic details of clinical drug APV binding to the wild-type and triple mutant HIV-1 protease. We have observed that the D atom of the catalytic site can be located at various positions, making conventional and low-barrier hydrogen bonding interactions with the catalytic aspartic acid residues and/or hydroxyl group of APV. Drug resistant mutations V32I, I47V and V82I do not seem to alter the hydrogen bonding pattern and hydrophobic interactions of amprenavir with the enzyme, even though the 100K X-ray crystal structure of PR_{TM}-APV suggests otherwise. Thus, our results reveal the limitations of the comparison of the HIV-1 PR structures obtained at 100K, suggesting that in certain cases mutations do not disrupt drug-enzyme contacts, and that in these cases other drug resistance mechanisms, such as global dynamics and conformational flexibility, may play a decisive role.

Experimental Section

General Information

Amprenavir (APV) and darunavir (DRV) were obtained through the NIH AIDS reagent program. The drugs were dissolved in dimethylsulfoxide (DMSO) at a final concentration of 20 and 40 mM, respectively. Protein purification supplies were purchased from GE Healthcare (Piscataway, New Jersey, USA). Crystallization reagents were purchased from Hampton Research (Aliso Viejo, California, USA).

Author Manuscript Author Manuscript Author Manuscript Author Manuscript

Protein expression and purification

The PR_{TM} has substitutions V32I, I47V and V82I associated with drug resistance, which are in addition to five stabilizing substitutions Q7K, L33I, L63I, C67A and C95A.[44,45] The expression and purification were performed using a methodology described previously,[17] in which the minimal medium made with 100 % D_2O and hydrogenous glycerol as the sole carbon source are used. *E. coli* bacteria (BL21-DE3) bearing the plasmid pET11a and the HIV-1 protease insert were grown in a bioreactor. Cells were induced overnight with 1mM IPTG before harvesting. The enzyme was isolated and purified from inclusion bodies in H_2O buffers by size-exclusion chromatography and HPLC. PR_{TM} was refolded with 25mM formic acid and buffer exchanged into 50 mM NaOAc, pH 5.0 in solutions made with 100% D_2O. This methodology produces the protease perdeuteration level of ~85% (after H/D exchange) as reported previously.[17]

Crystallization

PR_{TM} crystallizes with only one APV (or DRV) orientation in the active site. APV was mixed with 3.0 mg/mL enzyme in a molar ratio of 10:1. Crystals of the complex were grown in 300μL drops made by mixing the sample and the reservoir solution (0.1M MES, 0.9 M NaCl, pH 6.0 in H_2O) at a 1:1 ratio in the 9-well glass plate/sandwich box sitting drop setup. Crystals suitable for neutron diffraction measured ~0.2 mm^3. For the neutron structure determination, a crystal was mounted in a quartz capillary containing the reservoir solution made with 100% D_2O. Another crystal from the same crystallization drop that provided the crystal for neutron data collection was mounted in the same fashion for room-temperature X-ray data collection. The labile H atoms were allowed to exchange with D by v D_2O vapour for 4 weeks for both crystals before starting data collection.

X-ray and neutron data collection

Room temperature X-ray crystallographic data set was collected on a Rigaku HighFlux HomeLab instrument equipped with a MicroMax-007 HF X-ray generator and Osmic VariMax optics. The diffraction images were obtained using an R-Axis IV^{++} image plate detector. Diffraction data were collected, integrated, and scaled using the HKL3000 software suite.[46] The room-temperature X-ray structure of PR_{TM}-APV was solved by the molecular replacement method using phasing information from the structure with PDB code 3S43.[19] The room-temperature X-ray structure was refined using SHELX-97.[47]

Quasi-Laue neutron data to 2.2 Å resolution were collected from the 0.2 mm^3 PR_{TM}-APV crystal at pH 6.0 at room temperature on the LADI-III beamline at the Institut Laue-Langevin.[48] Images were collected from 3 different crystal orientations. At each orientation, the crystal was held stationary at different φ settings for each 20 hour exposure. The neutron data were processed using the Daresbury Laboratory *LAUE* suite program *LAUEGEN* modified to account for the cylindrical geometry of the detector.[49,50] The program *LSCALE* [51] was used to determine the wavelength-normalization curve using the intensities of symmetry-equivalent reflections measured at different wavelengths. No explicit absorption corrections were applied. These data were then merged in *SCALA*.[52] A summary of the experimental and refinement statistics is given in Table S1.

Author Manuscript Author Manuscript Author Manuscript Author Manuscript

Joint X-ray/Neutron (XN) structure refinement

The joint XN structure of the PR_{TM}-APV complex at pH 6.0 was determined using *nCNS*[21] and manipulated in *Coot*.[53] After initial rigid-body refinement, several cycles of positional, atomic displacement parameter, and occupancy refinement followed. The structures were checked for the correctness of side-chain conformations and water molecule orientations, which were built based on the F_O-F_C difference neutron scattering length density maps. The $2F_O$-F_C and F_O-F_C neutron scattering length density maps were then examined to determine the correct orientation of hydroxyl groups, and protonation states of the enzyme residues. The protonation states of some disordered side chains could not be obtained directly, and remained ambiguous. All water molecules were refined as D_2O. Initially, water oxygen atoms were positioned according to their electron density peaks, and then were shifted slightly in accordance with the neutron scattering length density maps. The level of H/D exchange at all positions was refined because of the ~85% perdeuteration level of the enzyme. Thus, all H positions in the protease, and labile H positions in APV, were modelled as D and then the occupancies of the D atoms were refined individually within the range of −0.56 to 1.00 (the scattering length of H is −0.56 times the scattering length of D). Before depositing the final structures to the PDB, a script was run that converts a record for the coordinates of D atom into two records corresponding to an H and a D atom partially occupying the same site, both with positive partial occupancies that add up to unity.

Isothermal titration calorimetry (ITC)

Titrations were performed in 50 mM sodium acetate buffer at 28 °C and pH 5.8 on a iTC200 microcalorimeter (Malvern Instruments Inc., Westborough, MA) using ~15 μM (as dimer) PR_{TM} and 150 μM APV. The protease dimer was dialyzed against the ITC buffer in the presence of 0.25% DMSO to compensate for the DMSO present in the titrant when diluting from an APV stock solution. For competitive inhibitors that bind at only one site, dissociation constants K_L ($1/K_{assoc}$) are equivalent to the inhibition constants measured by enzyme kinetics (K_i). Data was processed using the Origin ITC software.

Supplementary Material

Refer to Web version on PubMed Central for supplementary material.

Acknowledgments

This research at ORNL's Spallation Neutron Source was sponsored by the Scientific User Facilities Division, Office of Basic Energy Sciences, U.S. Department of Energy. The Office of Biological and Environmental Research supported research at Oak Ridge National Laboratory's Center for Structural Molecular Biology (CSMB), using facilities supported by the Scientific User Facilities Division, Office of Basic Energy Sciences, U.S. Department of Energy. The authors thank Institut Laue Langevin (beamline LADI-III) for awarded neutron beamtime. ITW was partly supported by NIH grant R01GM02920. Notice: This manuscript has been authored by UT-Battelle LLC under DOE Contract No. DE-AC05-00OR22725.

Abbreviations Used

HIV-1	human immunodeficiency virus type-1
APV	amprenavir

Author Manuscript Author Manuscript Author Manuscript Author Manuscript

PR HIV-1 protease

References

1. Mehellou Y, De Clercq E. Twenty-six years of anti-HIV drug discovery: Where do we stand and where do we go? J Med Chem. 2010; 53:521–538. [PubMed: 19785437]
2. Louis JM, Weber IT, Tozser J, Clore GM, Gronenborn AM. HIV-1 protease: Maturation, enzyme specificity, and drug resistance. Adv Pharm. 2000; 49:111–146.
3. Pokorna J, Machala L, Rezacova P, Konvalinka J. Current and novel inhibitors of HIV protease. Viruses. 2009; 1:1209–1239. [PubMed: 21994591]
4. Wlodawer A, Vondrasek J. Inhibitors of HIV-1 protease: A major success of structure-assisted drug design. Annu Rev Biophys Biomol Struct. 1998; 27:249–284. [PubMed: 9646869]
5. Ghosh AK, Anderson DD, Weber IT, Mitsuya H. Enhancing protein backbone binding - A fruitful concept for combating drug-resistant HIV. Angew Chem Int Ed. 2012; 51:1778–1802.
6. Weber IT, Kneller DW, Wong-Sam A. Highly resistant HIV-1 proteases and strategies for their inhibition. Future Med Chem. 2015; 7:1023–1038. [PubMed: 26062399]
7. Mitsuya H, Maeda K, Das D, Ghosh AK. Development of protease inhibitors and the fight with drug-resistant HIV-1 variants. Adv Pharmacol. 2008; 56:169–197. [PubMed: 18086412]
8. Weber IT, Agniswamy J. HIV-1 protease: structural perspectives on drug resistance. Viruses. 2009; 1:1110–1136. [PubMed: 21994585]
9. Ali A, Bandaranayake RM, Cai Y, King NM, Kolli M, Mittal S, Murzycki JF, Nalam MNL, Nalivaika EA, Özen A, Prabu-Jeyabalan MM, Thayer K, Schiffer CA. Molecular basis for drug resistance in HIV-1 protease. Viruses. 2010; 2:2509–2535. [PubMed: 21994628]
10. Liu F, Kovalevsky AY, Tie Y, Ghosh AK, Harrison RW, Weber IT. Effect of flap mutations on structure of HIV-1 protease and inhibition by saquinavir and darunavir. J Mol Biol. 2008; 381:102–115. [PubMed: 18597780]
11. Shen CH, Wang YF, Kovalevsky AY, Harrison RW, Weber IT. Amprenavir complexes with HIV-1 protease and its drug-resistant mutants altering hydrophobic clusters. FEBS J. 2010; 277:3699–3714. [PubMed: 20695887]
12. Agniswamy J, Shen CH, Aniana A, Sayer JM, Louis JM, Weber IT. HIV-1 protease with 20 mutations exhibits extreme resistance to clinical inhibitors through coordinated structural rearrangements. Biochemistry. 2012; 51:2819–2828. [PubMed: 22404139]
13. Hong L, Zhang XC, Hartsuck JA, Tang J. Crystal structure of an in vivo HIV-1 protease mutant in complex with saquinavir: insights into the mechanisms of drug resistance. Prot Sci. 2000; 9:1898–1904.
14. Kurinov IV, Harrison RW. The influence of temperature on lysozyme crystals. Structure and dynamics of protein and water. Acta Crystallogr. 1995; D51:98–109.
15. Fraser JS, van den Bedem H, Samelson AJ, Lang PT, Holton JM, Echols N, Alber T. Accessing protein conformational ensembles using room-temperature X-ray crystallography. Proc Natl Acad Sci U S A. 2011; 108:16247–16252. [PubMed: 21918110]
16. Keedy DA, van den Bedem H, Sivak DA, Petsko GA, Ringe D, Wilson MA, Fraser JS. Crystal cryocooling distorts conformational heterogeneity in a model Michaelis complex of DHFR. Structure. 2014; 22:899–910. [PubMed: 24882744]
17. Weber IT, Waltman MJ, Mustyakimov M, Blakeley MP, Keen DA, Ghosh AK, Langan P, Kovalevsky AY. Joint X-ray/neutron crystallographic study of HIV-1 protease with clinical inhibitor amprenavir: Insights for drug design. J Med Chem. 2013; 56:5631–5635. [PubMed: 23772563]
18. Kim EE, Baker CT, Dwyer MD, Murcko MA, Rao BG, Tung RD, Navia MA. Crystal structure of HIV-1 protease in complex with VX-478, a potent and orally bioavailable inhibitor of the enzyme. J Am Chem Soc. 1995; 117:1181–1182.
19. Tie Y, Wang YF, Boross PI, Chiu TY, Ghosh AK, Tozser J, Louis JM, Harrison RW, Weber IT. Critical differences in HIV-1 and HIV-2 protease specificity for clinical inhibitors. Prot Sci. 2012; 21:339–350.

Author Manuscript Author Manuscript Author Manuscript Author Manuscript

20. Blakeley MP, Hasnain SS, Antonyuk SV. Sub-atomic X-ray crystallography and neutron crystallography: promise, challenges and potential. IUCR J. 2015; 2:464–474.
21. Adams PD, Mustyakimov M, Afonine PV, Langan P. Generalized X-ray and neutron crystallographic analysis: more accurate and complete structures for biological macromolecules. Acta Crystallogr. 2009; D65:567–573.
22. Kovalevsky AY, Liu F, Leshchenko S, Ghosh AK, Louis JM, Harrison RW, Weber IT. Ultra-high resolution crystal structure of HIV-1 protease mutant reveals two binding sites for clinical inhibitor TMC114. J Mol Biol. 2006; 363:161–173. [PubMed: 16962136]
23. Hyland LJ, Tomaszek TA Jr, Meek TD. Human immunodeficiency virus-1 protease. 2. Use of pH rate studies and solvent kinetic isotope effects to elucidate details of chemical mechanism. Biochemistry. 1991; 30:8454–8463. [PubMed: 1883831]
24. Garrec J, Sautet P, Fleurat-Lessard P. Understanding the HIV-1 protease reactivity with DFT: What do we gain from recent functionals? J Phys Chem B. 2011; 115:8545–8558. [PubMed: 21667951]
25. Torbeev V, Yu, Kent SBH. Ionization state of the catalytic dyad Asp25/25′ in the HIV-1 protease: NMR studies of site-specifically ^{13}C labelled HIV-1 protease prepared by total chemical synthesis. Org Biomol Chem. 2012; 10:5887–5891. [PubMed: 22659831]
26. McGee TD Jr, Edwards J, Roitberg AE. pH-REMD simulations indicate that the catalytic aspartates of HIV-1 protease exist primarily in a monoprotonated state. J Phys Chem B. 2014; 118:12577–12585. [PubMed: 25340507]
27. Harrison RW, Weber IT. Molecular dynamics simulations of HIV-1 protease with peptide substrate. Protein Eng. 1994; 7:1353–1363. [PubMed: 7700867]
28. Piana S, Carloni P. Conformational flexibility of the catalytic Asp dyad in HIV-1 protease: An ab initio study on the free enzyme. Proteins: Struct, Funct Genet. 2000; 39:26–36. [PubMed: 10737924]
29. Piana S, Bucher D, Carloni P, Rothlisberger U. Reaction mechanism of HIV-1 protease by hybrid Car-Parrinello/Classical MD simulations. J Phys Chem B. 2004; 108:11139–11149.
30. Porter MA, Molina PA. The low-barrier double well potential of the $O^{\delta 1}$-H-$O^{\delta 1}$ hydrogen bond in unbound HIV protease: A QM/MM characterization. J Chem Theory Comput. 2006; 2:1675–1684. [PubMed: 26627038]
31. Northrop DB. Follow the protons: a low-barrier hydrogen bond unifies the mechanisms of the aspartic proteases. Acc Chem Res. 2001; 34:790–797. [PubMed: 11601963]
32. Gerlits O, Wymore T, Das A, Shen CH, Parks JM, Smith JC, Weiss KL, Keen DA, Blakeley MP, Louis JM, Langan P, Weber IT, Kovalevsky A. Long-range electrostatics-induced two-proton transfer captured by neutron crystallography in an enzyme catalytic site. Angew Chem Int Ed. 2016; 55:4924–4927.
33. Adachi M, Ohhara T, Kurihara K, Tamada T, Honjo E, Okazaki N, Arai S, Shoyama Y, Kimura K, Matsumura H, Sugiyama S, Adachi H, Takano K, Mori Y, Hidaka K, Kimura T, Hayashi Y, Kiso Y, Kuroki R. Structure of HIV-1 protease in complex with potent inhibitor KNI-272 determined by high-resolution X-ray and neutron crystallography. Proc Natl Acad Sci U S A. 2009; 106:4641–4646. [PubMed: 19273847]
34. Torbeev V, Yu, Raghuraman H, Hamelberg D, Tonelli M, Westler WM, Perozo E, Kent SBH. Protein conformational dynamics in the mechanism of HIV-1 protease catalysis. Proc Natl Acad Sci U S A. 2011; 108:20982–20987. [PubMed: 22158985]
35. Plevin MJ, Bryce DL, Boisbouvier J. Direct detection of CH/π interactions in proteins. Nat Chem. 2010; 2:466–471. [PubMed: 20489715]
36. King NM, Prabu-Jeyabalan M, Nalivaika EA, Wigerinck P, de Bethune MP, Schiffer CA. Structural and thermodynamic basis for the binding of TMC114, a next-generation human immunodeficiency virus type 1 protease inhibitor. J Virol. 2004; 78:12012–12021. [PubMed: 15479840]
37. Piana S, Carloni P, Rothlisberger U. Drug resistance in HIV-1 protease: flexibility-assisted mechanism of compensatory mutations. Prot Sci. 2002; 11:2393–2402.
38. Foulkes-Murzycki JE, Scott WRP, Schiffer CA. Hydrophobic sliding: A possible mechanism for drug resistance in human immunodeficiency virus type 1 protease. Structure. 2007; 15:225–233. [PubMed: 17292840]

Author Manuscript Author Manuscript Author Manuscript Author Manuscript

39. Cai Y, Yilmaz NK, Myint W, Ishima R, Schiffer CA. Differential flap dynamics in wild-type and a drug resistant variant of HIV-1 protease revealed by molecular dynamics and NMR relaxation. J Chem Theory Comput. 2012; 8:3452–3462. [PubMed: 23144597]
40. Meher BR, Patel S. Structural and dynamical aspects of HIV-1 protease and its role in drug resistance. Adv Prot Chem Struct Biol. 2013; 92:299–324.
41. de Vera IMS, Smith AN, Dancel MCA, Huang X, Dunn BM, Fanucci GE. Elucidating a relationship between conformational sampling and drug resistance in HIV-1 protease. Biochemistry. 2013; 52:3278–3288. [PubMed: 23566104]
42. Cai Y, Myint W, Paulsen JL, Schiffer CA, Ishima R, Yilmaz NK. Drug resistance mutations alter dynamics of inhibitor-bound HIV-1 protease. J Chem Theory Comput. 2014; 10:3438–3448. [PubMed: 25136270]
43. Shen CH, Chang YC, Agniswamy J, Harrison RW, Weber IT. Conformational variation of an extreme drug resistant mutant of HIV protease. J Mol Graphics Modell. 2015; 62:87–96.
44. Wondrak EM, Louis JM. Influence of flanking sequences on the dimer stability of human immunodeficiency virus type 1 protease. Biochemistry. 1996; 35:12957–12962. [PubMed: 8841142]
45. Mahalingam B, Louis JM, Hung J, Harrison RW, Weber IT. Structural implications of drug-resistant mutants of HIV-1 protease: high-resolution crystal structures of the mutant protease/substrate analogue complexes. Proteins. 2001; 43:455–464. [PubMed: 11340661]
46. Minor W, Cymborowski M, Otwinovski Z, Chruszcz M. HKL3000: The integration of data reduction and structure solution – from diffraction images to an initial model in minutes. Acta Crystallogr. 2006; D62:859–866.
47. Sheldrick GM, Schneider TR. High-resolution refinement. Methods Enzymol. 1997; 277:319–343. [PubMed: 18488315]
48. Blakeley MP, Teixeira SCM, Petit-Haertlein I, Hazemann I, Mitschler A, Haertlein M, Howard E, Podjarny AD. Neutron macromolecular crystallography with LADI-III. Acta Crystallogr. 2010; D66:1198–1205.
49. Campbell JW. LAUEGEN, an X-windows-based program for the processing of Laue diffraction data. J Appl Crystallogr. 1995; 28:228–236.
50. Campbell JW, Hao Q, Harding MM, Nguti ND, Wilkinson C. LAUEGEN version 6.0 and INTLDM. J Appl Crystallogr. 1998; 31:496–502.
51. Arzt S, Campbell JW, Harding MM, Hao Q, Helliwell JR. LSCALE - the new normalization, scaling and absorption correction program in the Daresbury Laue software suite. J Appl Crystallogr. 1999; 32:554–562.
52. Weiss MS. Global indicators of X-ray data quality. J Appl Crystallogr. 2001; 34:130–135.
53. Emsley P, Lohkamp B, Scott WG, Cowtan K. Features and development of Coot. Acta Crystallogr. 2010; D66:486–501.

Author Manuscript Author Manuscript Author Manuscript Author Manuscript

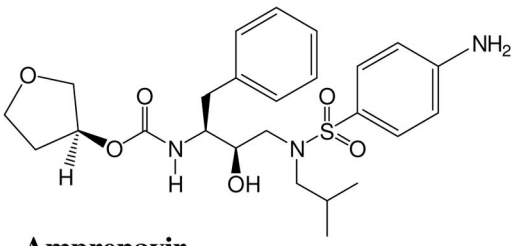

Amprenavir

A

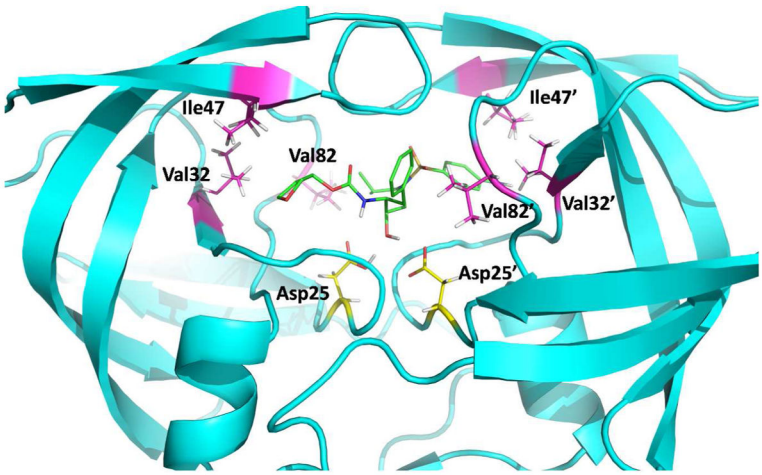

B

Figure 1.

(**A**) A chemical diagram of clinical HIV-1 PR inhibitor amprenavir (APV). (**B**) XN structure of the PR_{WT}-APV complex at pH 6.0 in cartoon representation, showing the locations of residues 32, 47, 82 and the catalytic aspartic acids, including D atoms shown in light grey (PDB ID 4JEC).

Author Manuscript Author Manuscript Author Manuscript Author Manuscript

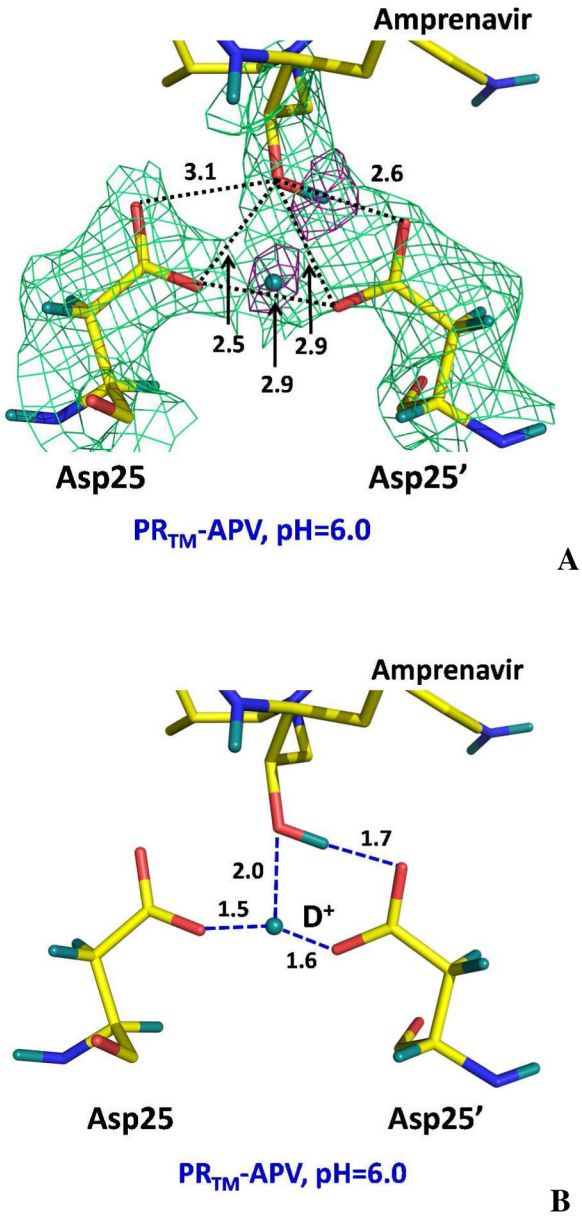

Figure 2.

Positions of D atoms in the HIV-1 PR catalytic site of PR_{TM}-APV complex at pH 6.0. (**A**) $2F_O$-F_C (green mesh, contoured at 1.0σ level) and omit difference F_O-F_C (violet mesh, contoured at 3.0σ level) neutron scattering length density maps for Asp25, Asp25′ of PR_{TM} and the hydroxyl group of APV. The omit map indicates the exact locations of D atoms in the catalytic site. O···O distances are shown as black dotted lines and are in Å. (**B**) D···O distances in Å shown as blue dashed lines between Asp25, Asp25′ and the hydroxyl group of APV.

Author Manuscript Author Manuscript Author Manuscript Author Manuscript

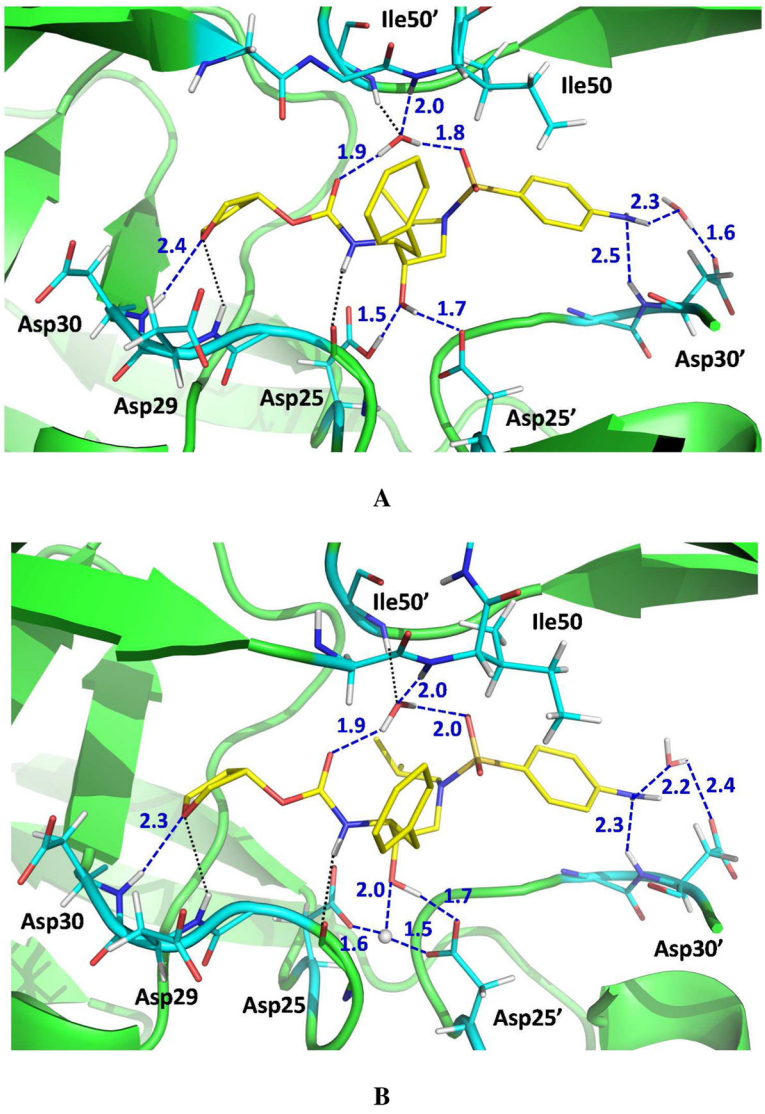

Figure 3.

Hydrogen bonding interactions (blue dashed lines) in PR_{WT}-APV **(A)** and PR_{TM}-APV **(B)** XN structures. Interactions suggested by previous low temperature X-ray structures, but considered weak or absent from the XN structures are shown as black dotted lines. Distances are in Å.

Author Manuscript Author Manuscript Author Manuscript Author Manuscript

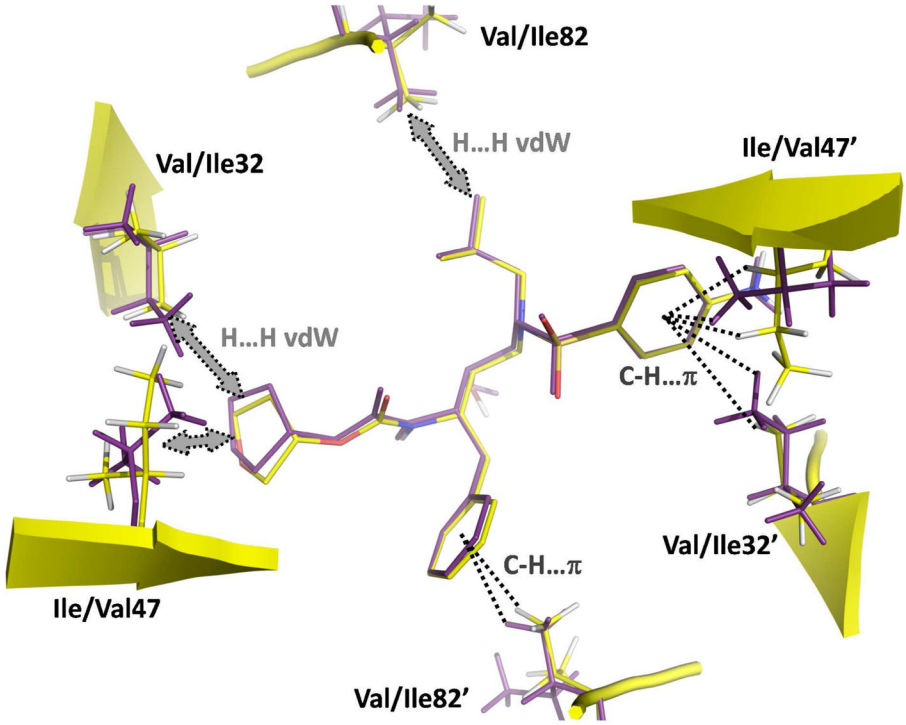

Figure 4.

Superposition of the PR_{TM}-APV (violet, PDB ID 5T8H) and PR_{WT}-APV (yellow carbon, PDB ID 4JEC) neutron structures, showing the mutation sites and hydrophobic interactions.

Author Manuscript Author Manuscript Author Manuscript Author Manuscript

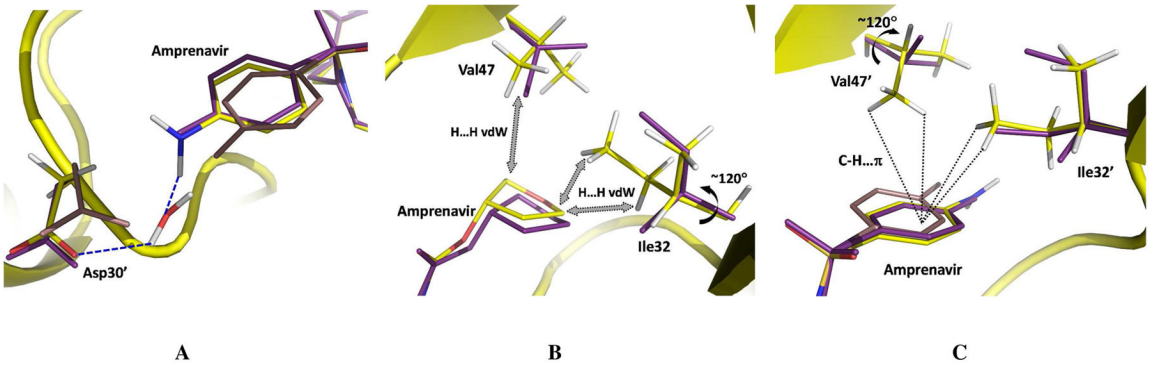

Figure 5.

Superposition of the room temperature XN (yellow carbons, PDB ID 5T8H) and 100K X-ray (violet, brown for disordered groups, PDB ID 3S43) structures of PR_{TM}-APV showing APV-enzyme interactions. **A)** Hydrogen bonding and water-mediated interactions between the aniline group and Asp30′; **B)** van der Waals contacts made by the tetrahydrofuran moiety with Ile32 and Val47; **C)** C-H···π contacts made by the aniline group with Ile32′ and Val47′.